ELSEVIER

Nuclear Engineering and Design 146 (1994) 349–362

Nuclear Engineering and Design

Solid breeder thermal transient under purge-line-break accidents

Alice Y. Ying, Mohamed A. Abdou

Mechanical, Aerospace and Nuclear Engineering Department, 43–133 Engineering IV, University of California, Los Angeles, Los Angeles, CA 90024-1597, USA

Abstract

The breeder thermal performances under a purge line break have been analyzed for two blanket design options: a blanket design using a packed breeder bed and a blanket design using a sintered breeder product. Under a purge line break open to a vacuum environment, the packed bed breeder temperature exceeds its operating temperature limit at a faster rate than that of the sintered breeder blanket design for the same breeder temperature gradient. Depending on the breeder material and nominal operating conditions, the breeder reaches its maximum operating temperature in time ranging from 32 seconds to 125 seconds for a break area of 10 cm^2 in packed bed designs. However for the sintered product design, the consequence of this transient might not result in the breeder exceeding its maximum operating temperature if a reasonable contact pressure could be established at the interface. To reduce the safety hazards, the tritium concentration build up in the vacuum vessel in conjunction with the purge gas pressure inside the blanket module should be used as a measure for initiating the reactor shutdown for this type of accident. The consequence of the purge line break outside the vacuum vessel on the breeder transient thermal performance is less significant because of a longer transient time involved.

1. Introduction

The prediction of the temperature magnitude and gradient across a breeder region is of concern to blanket design engineers due to the limited operating temperature window for the breeder materials. This problem is even more complicated when a thermal gap conductance is involved or the thermal properties of the region becomes a function of the surrounding environment. The purge helium gas running through the breeding zone serves as a carrier for tritium removal. Even if it does not transport a significant amount of heat, it plays an important role in the determination of the thermal operating condition of the breeding zone because of its effect on the thermal conductance of the porous ceramic breeder.

Though no detailed design layout has been proposed for a solid breeder blanket purge gas system, the purge gas system inside the vacuum vessel might look similar to the cooling system, which utilizes common ring ducts to serve as inlet and outlet manifolds. The gas enters/leaves each blanket sector through tubes connected to these ducts. Since a reactor blanket might have 32 or 48 blanket sectors, it is then expected that 32 or 48 purge gas tubes will join with each manifold. A schematic view of a tokamak reactor (ITER) showing the vacuum vessel, blanket and shield components is given in Fig. 1 [1]. For this

0029-5493/94/$07.00
SSDI 0029-5493(93)E0241-B

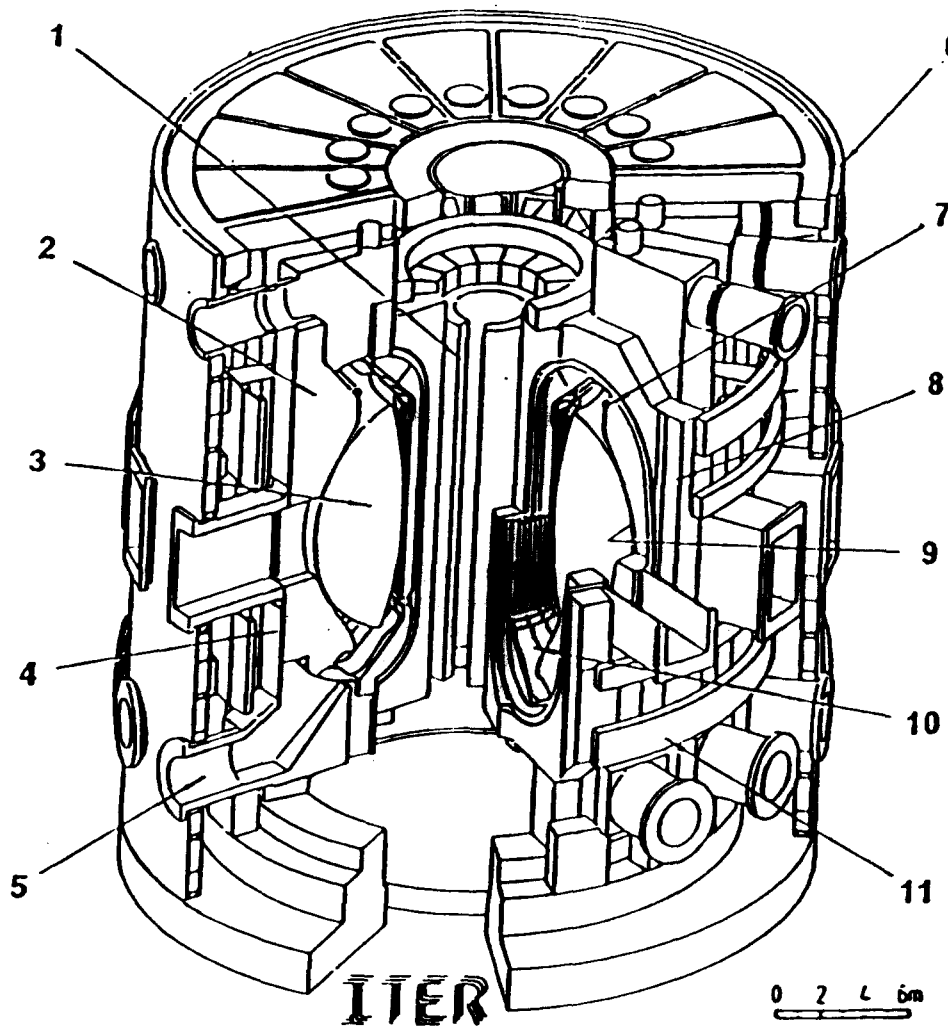

1- CENTRAL SOLENOID
2- SHIELD/BLANKET
3- PLASMA
4- VACUUM VESSEL SHIELD
5- PLASMA EXHAUST
6- CRYOSTAT
7- ACTIVE CONTROL COILS
8- TOROIDAL FIELD COILS
9- FIRST WALL
10- DIVERTOR PLATES
11- POLOIDAL FIELD COILS

Fig. 1. Schematic view of ITER device showing vacuum vessel, blanket/shield and other reactor components.

machine, the operating pressure inside the vacuum vessel is set at 1×10^{-5} mbar. Outside the vacuum vessel, the pressure is set at 1 bar absolute. The vacuum vessel is equipped with tritium monitors and remote leak detectors.

In this work, the breeder temperature transients under a purge line break open to the vacuum vessel and outside are studied. The consequences for different design concepts are evaluated. It is hoped that

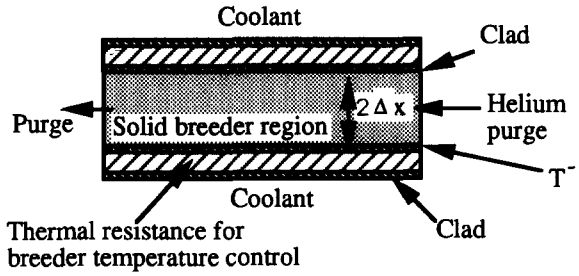

Fig. 2. Typical slab configuration of a solid breeder blanket design.

the results of this study will provide blanket design engineers with an insight into the detailed design features needed to mitigate this type of accident.

2. Solid breeder temperature

The solid breeder temperature, which dictates the tritium inventory, is directly dependent on the overall thermal conductance between the coolant and breeder. Its mean value in a slab geometry (see Fig. 2) under a transient condition can be written as [2]:

$$\frac{d\bar{T}(t)}{dt} = \frac{1}{\rho C_p}\left(q''' - \frac{(\bar{T}(t) - T^-)}{R}\right), \tag{1}$$

where T^- is the inner clad surface temperature, ρ is the density of the breeder, C_p is the specific heat of the breeder, and $1/R$ is the overall thermal conductance of the breeder region. Since the purge gas only runs through the breeder region, the thermal resistance between the coolant and breeder clad is not affected under this type of accident. Therefore, T^- can be seen as a constant value if there are no other changes in the operating conditions.

Depending on the design configuration, the overall thermal conductance is a function of the thermal conductances of the breeder material (in either packed bed or sintered block forms) and of the solid breeder/clad interface.

2.1. Thermal conductance of a packed breeder bed

One material configuration considered in the solid breeder blanket design is in sphere-pac pebble, from which a packed breeding bed is formed. The heat transfer in the interior of packed beds with fluid flow (the helium purge) is determined by the characteristics of the heat transport in the bulk and near the wall regions. The heat transport in the bulk region can either be convective dominated or conductive dominated depending upon the gas Peclet number Pe_0. The transition from conductive to mixing-controlled convective heat transfer can be detected by a critical value of the Peclet number. In the case of heat transfer in packed beds with a gaseous fluid phase, values of the critical Peclet number between 30 and 300 were obtained by Tsotasas and Schlünder [3]. For the solid breeder blanket design, the helium purge flow rate in the breeder region is determined by the maximum allowable tritium partial pressure in the purge. The tritium partial pressure is considered as a key parameter because of its important relationship with tritium permeation and inventory. Estimations of the gas Peclet number for the ITER packed bed design are 0.022 and 0.0022 for tritium partial pressures of 10 and 100 Pa, respectively [4].

Thus, for blanket design calculations, the effect of flow on the packed bed thermal conductivity can be neglected.

The effective thermal conductivity of a packed bed $\bar{\lambda}_{bed}$ without fluid flow was obtained by Bauer and Schlünder [5]:

$$\frac{\bar{\lambda}_{bed}}{\lambda_g} = \left(1-\sqrt{1-\varphi}\right)\left(\frac{\varphi}{\varphi-1+\lambda_g/\lambda_D}+\varphi\frac{\lambda_R}{\lambda_g}\right)+\sqrt{1-\varphi}\left(\phi\frac{\lambda_s}{\lambda_g}+(1-\phi)\frac{\lambda^*}{\lambda_g}\right), \tag{2}$$

where

$$\frac{\lambda^*}{\lambda_g} = \frac{2}{(N-M)}\left[\frac{B\left(\frac{\lambda_s}{\lambda_g}+\frac{\lambda_R}{\lambda_g}-1\right)\frac{\lambda_g}{\lambda_D}\Big/\frac{\lambda_s}{\lambda_g}}{(N-M)^2}\ln\left(\frac{\left(\frac{\lambda_s}{\lambda_g}+\frac{\lambda_R}{\lambda_g}\right)\frac{\lambda_g}{\lambda_D}}{B\left[1+\left(\frac{\lambda_g}{\lambda_D}-1\right)\left(\frac{\lambda_s}{\lambda_g}+\frac{\lambda_R}{\lambda_g}\right)\right]}\right)\right.$$

$$\left.-\frac{B-1}{N-M}\frac{\lambda_g}{\lambda_D}+\frac{B+1}{2B}\left(\frac{\lambda_R}{\lambda_g}\frac{\lambda_g}{\lambda_D}-B\left[1+\left(\frac{\lambda_g}{\lambda_D}-1\right)\frac{\lambda_R}{\lambda_g}\right]\right)\right], \tag{3}$$

$$N-M = \left[1+\left(\frac{\lambda_R}{\lambda_g}-B/\frac{\lambda_g}{\lambda_D}\right)\Big/\frac{\lambda_s}{\lambda_g}\right]\frac{\lambda_g}{\lambda_D}-B\left(\frac{\lambda_g}{\lambda_D}-1\right)\left(1+\frac{\lambda_R}{\lambda_g}\Big/\frac{\lambda_s}{\lambda_g}\right), \tag{4}$$

$$\frac{\lambda_R}{\lambda_g} = \frac{0.04\sigma}{(2/\epsilon-1)\lambda_g}\left(\frac{T}{100}\right)^3 D_p, \tag{5}$$

φ = porosity, ϕ = fractional contact area, ϵ = emissivity, σ = the Stephan-Boltzmann constant.

The influence of gas pressure on the effective thermal conductivity of a packed bed is through the Smoluchowski effect [5]. This results in an additional wall heat-transfer resistance appearing in the region around the particle contact points. This resistance is reflected in defining an equivalent thermal conductivity of gas λ_D as a function of the mean free path of the gas molecules l_t and the effective gas path that characterizes the size of the gas space X_D:

$$\frac{\lambda_g}{\lambda_D} = 1+\frac{2l_t}{X_D}\left(\frac{2}{\alpha}-1\right), \tag{6}$$

where α is the thermal accommodation coefficient of the fill gas. The mean free path of the gas at temperature T and pressure P, l_t, is given as a function of gas Prandtl number Pr and specific heat ratio γ:

$$l_t = 2\frac{\gamma}{\gamma+1}\frac{1}{\mathrm{Pr}}\frac{P_{STP}}{P}\frac{T}{273}l_0 \tag{7}$$

and X_D is equal to the particle diameter (D_p) as suggested in Ref. [5].

The model of the packed bed wall heat transfer coefficient proposed by Yagi and Kunii [6] was modified to take account of the gas pressure effect. This model assumes that the total heat flux through the near-wall region (half of particle diameter) is the sum of the heat flux in the void space and heat flux in the effective solid phase. Similar to the packed bed effective thermal conductivity, the pressure of a

gas substantially affects its conductivity if the gas in the void region is in the Smoluchowski region. For this situation, the gas characteristic distance is small as compared to the mean free path of the gas molecules, and the thermal conductivity of gas can be estimated by using Eq. (6). The resulting packed bed wall heat transfer coefficient, by neglecting the effect of thermal radiation, is written as:

$$h_w = \left(\frac{1}{1/(\lambda_w/\lambda_g) + 0.5(\bar{\lambda}_{bed}/\lambda_g)} \right) \lambda_g / D_p, \tag{8}$$

where

$$\frac{\lambda_w}{\lambda_g} = \varphi_w \left(\frac{2}{1 + \frac{4l_t}{D_p}\left(\frac{2}{\alpha} - 1\right)} \right) + \frac{1 - \varphi_w}{1/\left\{ \frac{1}{\phi_w} + 1/\left[1 + \frac{4l_t}{D_p}\left(\frac{2}{\alpha} - 1\right) \right] \right\} + \frac{\lambda_g}{3\lambda_s}}, \tag{9}$$

where

$$\phi_w = \frac{1}{4} \frac{((\lambda_r - 1)/\lambda_r)^2}{\ln \lambda_r - (\lambda_r - 1)/\lambda_r} - \frac{1}{3\lambda_r} \tag{10}$$

and λ_r is the conductivity ratio of the solid to the gas:

$$\lambda_r = \lambda_s / \lambda_g. \tag{11}$$

In Eq. (9), a void fraction of 70% is assumed for φ_w. The overall thermal conductance of the breeder packed bed is written as:

$$h = \frac{1}{R} = \frac{1}{\Delta x / 3\bar{\lambda}_{bed} + 1/h_w}, \tag{12}$$

where Δx is the breeder bed half-width.

2.2. Thermal conductance of a sintered breeder zone

Another breeder material form considered is sintered block. Heat transfer across the sintered breeder/clad interface is usually accompanied by a measurable temperature drop due to the thermal resistance in this region. The contribution of the purge gas to the sintered breeder temperature behavior comes from this interfacial thermal resistance.

The thermal contact conductance at the interface is formulated in terms of material properties, surface characteristics and the contact pressure at the interface as indicated in Ref. [7]:

$$h_c = \frac{\lambda_g}{(\delta_s + \delta_c) + (\zeta_s + \zeta_c)} + 2\lambda_m \frac{1}{a(\delta_c^{1/2})} \frac{P_c}{H_s} + \frac{\sigma}{\frac{1}{\epsilon_s} + \frac{1}{\epsilon_c} - 1} (T_s^2 + T_c^2)(T_s + T_c), \tag{13}$$

where δ is the rms roughness and the jump distance (ζ) for Maxwell molecules is written as

$$\zeta_s + \zeta_c = 2.171 \times 10^{-10} \tilde{T}^{1.29} / P. \tag{14}$$

Under a vacuum environment, Eq. (13) indicates that the thermal contact conductance depends on the contact pressure, P_c. The overall thermal conductance of the breeder sintered product zone in a plate geometry is written as:

$$h = \frac{1}{R} = \frac{1}{\Delta x / 3\lambda_s + 1/h_c}. \tag{15}$$

3. Purge gas depressurization transient

Once a break occurs in the purge gas line, a substantial loss of the purge gas inventory is incurred. The analysis assumes that the flow can be described as a perfect gas. Since the purge gas is to be discharged into a vacuum environment, the fluid speed at the break point reaches its sonic velocity and a choked flow exists. In addition, because of the reactor vacuum vessel having a much larger volume compared to the purge gas inventory, it is adequate to assume that the choked flow exists over the depressurization transient. This gives [8]:

$$\frac{C_b}{C_o} = \sqrt{\frac{2}{\gamma+1}}, \tag{16}$$

$$\frac{\rho_b}{\rho_o} = \left(\frac{2}{\gamma+1}\right)\frac{1}{\gamma-1}, \tag{17}$$

$$C_o = \sqrt{\gamma RT}, \tag{18}$$

and the Mach number, M, at the exit condition is equal to 1;

$$M = v_b/C_b = 1, \tag{19}$$

where the subscript o represents the gas conditions inside the blanket module, and the subscript b corresponds to the conditions at the break point. The transient purge gas depressurization can be estimated from the mass balance equation:

$$\frac{d\rho V}{dt} = -W = -\rho_b v_b A. \tag{20}$$

The gas properties at break conditions can be replaced by the vessel quantities, and by using the perfect gas law to eliminate the density from the above equation, we have:

$$\frac{d(P/T)}{dt} = -\frac{A}{V}\frac{P}{T}\left(\frac{2}{\gamma+1}\right)\frac{1}{\gamma-1}\sqrt{\frac{2}{\gamma+1}}\sqrt{\gamma RT}, \tag{21}$$

where P, T are the purge gas pressure and temperature, respectively.

The purge gas temperature increases with the breeder temperatures following the depressurization transient. This is due to a reduction of the effective thermal conductance of the breeder zone. Because of the low heat capacity of the gas, the gas temperature as a function of time is assumed to be equal to the mean solid breeder temperature as the case assumed for the homogeneous model and calculated by Eq. (1).

4. Results

4.1. Packed breeder bed design

Example calculations were performed for two blanket design concepts. In case 1, an ITER blanket pebble design option was assumed [9]. This design utilizes a single size breeder (Li_2O) pebble with a particle diameter of 1 mm forming a 60% dense packing. The maximum allowable operating temperature for this material is set at 1000°C in the present calculation (In general, the maximum temperature is set at the temperature at which the sintering becomes significant.). The nuclear heat generation closest to the plasma side is about 18.5 W/cm^3 for the breeder with 50% ^{6}Li enrichment. Given this nuclear heat

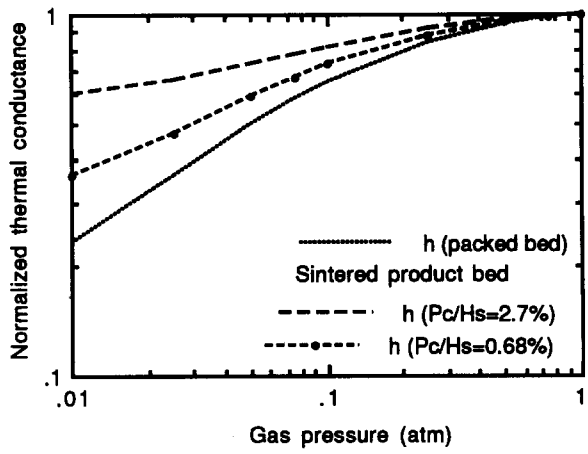

Fig. 3. The effect of gas pressure on normalized breeder zone thermal conductances for different blanket design concepts.

generation rate and the effective thermal conductivity of 1.48 W/mK, the front zone breeder temperature difference is about 206°C for a radial thickness of 1.15 cm. The overall purge helium gas volume inside the blanket modules is of the order of 18 m^3. The effect of gas pressure on this breeder packed bed thermal conductance is shown in Fig. 3. It indicates that the bed thermal conductance decreases by a factor of 2 as the gas pressure decreases from 1 to 0.005 MPa.

In case 2, calculations were performed for a reactor-type blanket design: ARIES-I. [10]. For this design, the breeding zone consists of a coarse beryllium packed bed mixed with fine Li_2ZrO_3 breeder particles. The size of the beryllium particle is 1 mm, while the size of the breeder particle is 0.1 mm. The packing fraction of the breeding zone is about 80% where 60% of packing comes from beryllium particles. Typical breeding zone thickness for this design is 1.1 cm with the maximum nuclear heating rate of 29.8 W/cm^3. The overall purge helium gas volume inside the blanket modules is about 12 m^3. The evaluation of such a binary bed consists first of determining the effective thermal conductivity of the fine breeder particle bed and then substituting this effective thermal conductivity to the filled space of

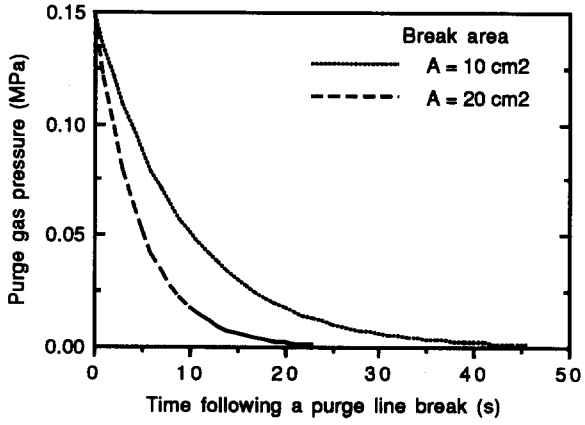

Fig. 4. Example calculations of packed bed purge gas pressure histories following a purge line break open to the vacuum environment.

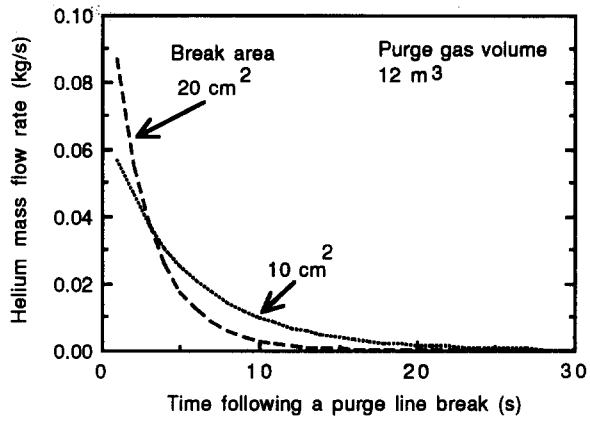

Fig. 5. Helium gas mass flow rate histories following a purge line break open to vacuum for different break areas. The purge gas volume inside the blanket module is 12 m^3.

the coarse beryllium bed. This method gives the breeding zone effective thermal conductivity of 7.0 W/mK, which is about 50% higher than the number indicated in the ARIES-I report (4.68 W/mK) [10]. (At present stage, there is no experimental data or realistic model to quantify which method is more accurate.) During the transient calculation, the calculated effective thermal conductivity is normalized by a factor of 1.5 to be consistent with the ARIES-I steady state thermal calculations.

The results of purge gas pressure histories is shown in Fig. 4 for break areas of 10 and 20 cm^2. The gas pressure drops significantly at the beginning of the accident and then stays quite flat during the following time as shown in Fig. 4. This behavior can be seen if a constant gas temperature is assumed in Eq. (20). Integrating Eq. (20) one can show that the pressure inside the blanket module drops exponentially with time. A similar type of behavior can be seen in the transient helium mass flow rate histories. As shown in Fig. 5, the initial gas mass flow rate for a break area of 20 cm^2 is 9.0×10^{-2} kg/s while the mass flow rate at 16 seconds following the accident is about 2.38×10^{-4} kg/s. These results indicate that if the contained tritium is to be released with the purge gas, the tritium build up histories in the vacuum vessel

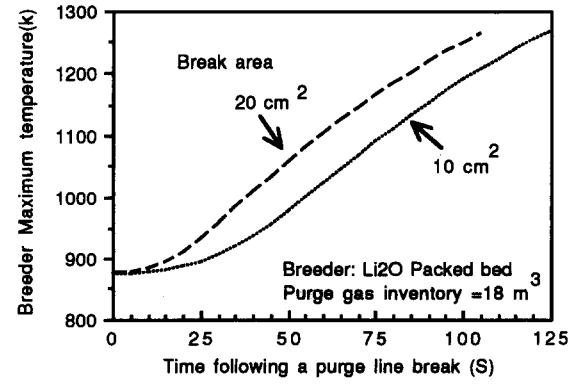

Fig. 6. Example calculations of packed bed breeder maximum temperature histories following a purge line break open to the vacuum environment.

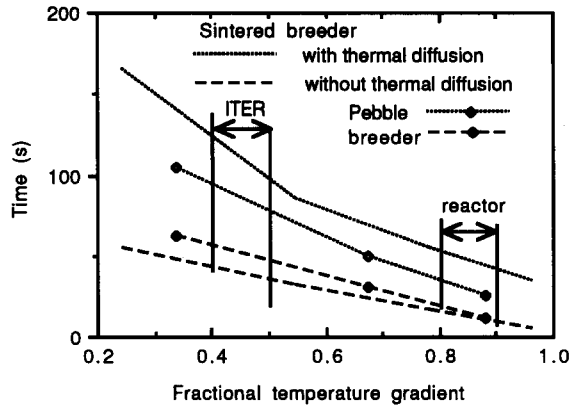

Fig. 7. Time for the breeder reaching its maximum temperature as a function of different fractional temperature gradients for different design concepts.

would follow the similar exponential behavior of the gas depressurization and increase rapidly at the beginning of the accident.

The breeder maximum temperature histories for ITER packed bed design are shown in Fig. 6. The calculations show that the breeder reaches its maximum temperature of 1000°C at about 105 and 125 seconds following the accident for break areas of 20 cm^2 and 10 cm^2, respectively. For both cases, an initial breeder maximum temperature of 600°C is assumed. (In ITER blanket designs, the breeder temperatures are chosen to lie in the lower part of the window of 400–1000°C to allow a margin for operating at a higher wall loading.) As shown in the figure, the breeder temperature does not increase significantly at the beginning of the accident. This is due to the amount of purge gas pressure inside the breeder that enables the thermal diffusion to transport the heat into the coolant. Once the purge gas pressure falls below 0.01 MPa, the breeder may be considered to behave essentially adiabatically and the breeder temperature increases linearly. (At this condition, the breeder behaves similar to the situation under a complete loss-of-coolant accident.) The breeder temperature as a function of time can be estimated from Eq. (1) by dropping the conduction term:

$$\frac{d\tilde{T}(t)}{dt} = \frac{q'''}{\rho C_p}. \tag{22}$$

The time for the breeder to heat up adiabatically to its maximum value can be determined from the aforementioned equation and is shown in Fig. 7 as a function of the fractional temperature gradient (f) which is defined as:

$$f = \Delta T_{\text{Nominal}} / \Delta T_{\text{maximum allowable}}. \tag{23}$$

The results for the ITER packed bed design indicate that the attainment of maximum breeder temperature is delayed substantially when compared to the case of a complete loss-of-coolant accident. This is due to the availability of thermal diffusion before the purge gas pressure falls below the value where the thermal conductance is independent of the gas pressure.

For a reactor type blanket, the coolant temperature is set as high as possible for power producing purpose. In addition, the high neutron wall load results in a higher nuclear heat generation rate when compared to that of the ITER blanket. Consequently, the breeder operating temperatures tend to be at the higher end of the temperature window. The result of a pure line break is then more serious due to the smaller temperature margin available for the breeder. Figure 8 illustrates the breeder maximum

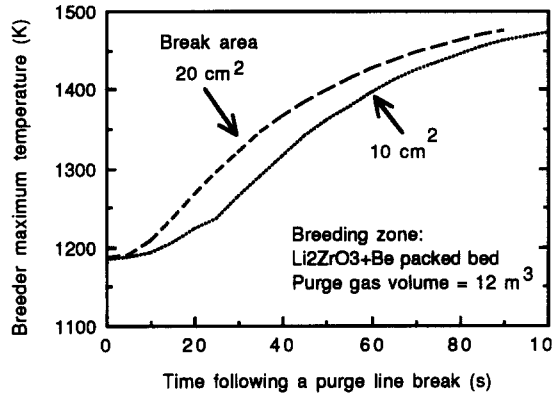

Fig. 8. Breeder maximum temperature histories following a purge line break open to vacuum for ARIES-I design.

temperature histories following a purge line open to the vacuum environment for the ARIES-I design. The analysis indicate that the breeder reaches its maximum temperature of 1000°C at about 21 and 32 seconds for break areas of 20 cm^2 and 10 cm^2, respectively. (Initial breeder maximum temperature is 907°C.) For this design, the time needed to heat up the breeder to its maximum temperature adiabatically is about 11 seconds. As shown in Fig. 8, if the maximum allowable temperature is 1200°C, the time to reach this value is approximately equal to 90 seconds.

4.2. Sintered product design

In general, a blanket design using a sintered breeder material will have less purge gas inventory because of the small purge channel being used in the breeder region. For example, this type of design for an ITER-type device has a purge gas inventory of 0.02 m^3 inside the blanket modules. This small purge gas inventory results in a rapid depressurization once the purge line opens to the vacuum environment. The merit of the sintered breeder product design under this type of transient is that the gas pressure only influences the breeder thermal behavior at the interface region. As shown in Fig. 2, for a ratio of contact pressure (P_c) to hardness (H_s) equal to 2.7% the overall normalized thermal conductance of a sintered product bed drops 40% at a gas pressure of 0.001 MPa, while for the same gas pressure, the normalized thermal conductance for a packed bed decreases by a factor of 4. Values of 50 μm and 1.8 μm are used for δ_s and δ_c, respectively, in the present calculation.

The calculated results of the breeder maximum temperature histories following the accident for different contact pressures are shown in Fig. 9 for a break size of 1 cm^2 and purge gas volume of 1 m^3 (by considering the inclusion of the gas inventory in the manifold region). The transient temperature calculations indicate that if a reasonable amount of contact pressure could be established at the breeder/clad interface, the breeder temperature would not exceed its temperature window under a purge gas depressurization transient. For the case shown the final maximum breeder temperature is about 780°C following the accident for a contact pressure of 4 MPa. (The compressive failure stress for the non-irradiated 80% TD Li_2O at 400°C is about 30 MPa [11].). If the breeder/clad contact pressure falls below this number, the ultimate thermal conductance results in the breeder temperature exceeding its maximum value at about 165 s following a purge line break for a contact pressure of 1 MPa. For the case assumed, the gas pressure falls below 0.01 MPa at about 25 seconds following the accident.

The time to reach the breeder's maximum temperature as a function of fractional temperature gradient for the sintered breeder design is also shown in Fig. 7. The results indicate that the effect of

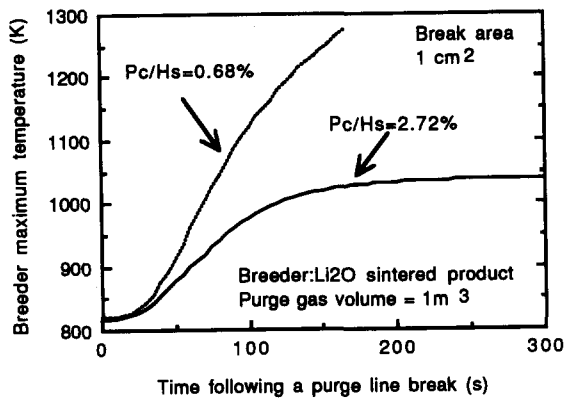

Fig. 9. Breeder maximum temperature histories following a purge line break open to the vacuum for different contact pressures ($H_s = 147$ MPa).

thermal diffusion delay the severity of the transient. This delay is more pronounced in the sintered block design when compared to the packed bed design. However, for all the cases considered, the purge line break open to the vacuum transient can be considered a slow transient (the time available for reactor shutdown being much greater than 10 seconds) with respect to the breeder temperature behavior.

5. Time-dependent gas exchange flow

If the purge line break occurs outside the vacuum vessel, the helium purge gas is to be exchanged with the filled gas which might be an inert gas or atmosphere. For this situation, the gas flow is driven by the density difference between the gas inside the blanket module and the gas outside the vessel. An experimental study of helium-air gas exchange flow has been carried out at JAERI [12], and the results of the exchange flow rate (Q) were presented in terms of densimetric Froude number, Fr:

$$\mathrm{Fr} = \frac{4Q}{\pi}\left[\frac{\rho_m}{D^5 g(\rho_h - \rho_c)}\right]^{0.5}. \tag{24}$$

For a 2 cm diameter of the cylindrical opening, the largest Fr number of 0.24 was obtained. The exchange mass flow rate at this Fr number is about 3.15×10^{-6} kg/s, which is on the order of 4 magnitudes less than that of a purge line break open to the vacuum environment. (Notice that the gas exchange flow rate decreases as the time increases due to a reduction of the density difference.) For this type of flow rate, the gas exchange flow transient might take few thousand seconds before it would reach an equilibrium state. The ultimate breeder packed bed thermal conductance decreases by a factor of 3, while the helium purge gas is fully replaced by the air. The breeder temperature reaches its operating limit if the bed thermal conductance decreases by a factor of two.

6. Summary

The breeder thermal response under a purge line break open to a vacuum environment has been analyzed in this paper. The breeder thermal behavior under a total loss of gas pressure is similar to that under a complete loss-of-coolant accident. However in this case, the rate of the breeder temperature

increase is suppressed at the beginning of the accident because of the effect of the thermal diffusion. This suppression rate is more pronounced for the sintered breeder design when compared with the packed bed design. Depending on the breeder material and nominal operating conditions, the breeder reaches its maximum operating temperature in time ranging from 32 seconds to 125 seconds for a break area of 10 cm^2 in packed bed designs. This indicates that this type of transient could be considered slow (the time available for initiating the reactor shutdown being more than 10 seconds) with respect to the breeder thermal response. For the sintered product design, the consequence of this transient might not result in the breeder exceeding its maximum operating temperature if a reasonable contact pressure could be established at the interface. The required contact pressure to meet this criterion depends on the ratio of the gap temperature drop to the bulk temperature difference. For a ratio of 1/4, the required contact pressure is 4 MPa for a hardness of 147 MPa. If the contained tritium is to be released with the purge gas, the tritium build up histories in the vacuum vessel would follow the similar exponential behavior of the gas depressurization and increase rapidly at the beginning of the accident. To reduce the safety hazards, the tritium concentration build up in the vacuum vessel in conjunction with the purge gas pressure inside the blanket module should be considered as a measure for initiating the reactor shutdown for this type of accident. The consequence of the purge line break outside the vacuum vessel on the breeder transient thermal performance is less significant because of a longer transient time involved. Due to increased interest in using a mixed (different conductivities and different particle sizes) binary bed in the blanket design, further experimental/modeling efforts on the heat transport phenomena of such a packed bed are needed.

7. Acknowledgment

This work was performed under U.S. Department of Energy Contract DE-FG03-86ER52123.

8. Nomenclature

a $= 0.1\ m^{1/2}$,
A break area,
B $= 1.25\ [(1-\varphi)/\varphi]^{10/9}$ for sphere,
C sonic velocity,
C_p specific thermal capacity, J/kgK,
D break opening diameter,
D_p particle diameter, m,
Fr densimetric Froude number defined by Eq. (24),
g acceleration of gravity,
H_s material hardness (= 147 MPa),
h heat transfer coefficient,
l_0 mean-free-path of gas molecules at 0.1013 MPa and 273 K,
l_t mean-free-path of gas molecules,
P gas pressure, MPa,
P_c contact pressure,
Pr Prandtl number,
P_{STP} = 0.1013 MPa,
Q exchange flow rate,

q''' volumetric heat generation rate,
R gas constant,
T temperature,
V gas inventory, m^3,
v gas velocity.

Greek

λ thermal conductivity, W/mK,
λ_m $= 2\ \lambda_s\lambda_c/(\lambda_s + \lambda_c)$,
μ viscosity, kg/ms,
ρ density, kg/m^3,
φ porosity,
γ $= c_p/c_v$,
ϕ fractional contact area,
α thermal accommodation coefficient of the fill gas,
Δx bed half-width,
δ the rms roughness height,
ϵ emissivity,
σ the Stephan-Boltzmann constant.

Subscripts

bed packed bed,
b break point,
c clad or cold,
crit critical value,
g gas,
h hot,
m mixture,
o inside the breeder module,
s solid breeder,
w wall.

9. References

[1] E. Salpietro, ITER: Engineering Basis, IAEA-CN-53/F-1-4 (1990).
[2] A.Y. Ying, R.A. Raffray, and M.A. Abdou, LOFA analysis for US ITER solid breeder blanket, Fusion Technology 19(3) Part 2B (1991) 1481–1486.
[3] E. Tsotsas and E.U. Schlünder, Heat transfer in packed beds with fluid flow: Remarks on the meaning and the calculation of a heat transfer coefficient at the wall, Chem. Engng. Sci. 45 (1990) 819–837.
[4] A.Y. Ying, R.A. Raffray, and M.A. Abdou, Helium purge flow analysis for EC and Japanese solid breeder blanket design for ITER, U.S. Contributions to the ITER Blanket Homework Task of Winter 1990 Session, ITER-TN-BL-5-0-3 (January–March 1990).
[5] R. Bauer and E.U. Schlunder, Effective radial thermal conductivity of packings in gas flow. Part II. Thermal conductivity of the packing fraction without gas flow, Int. Chemical Engineering 18, No. 2 (1978) 189–203.
[6] S. Yagi and D. Kunii, Studies on heat transfer in packed beds, 1961 Int. Heat Transfer Conf., Int. Developments in Heat Transfer, Part IV (1961) 750–759.

[7] M.A. Abdou et al., A demonstration tokamak power plant study (DEMO), ANL/FPP-82, Argonal National Laboratory (1982).
[8] P. Thompson, Compressible Fluid Dynamics (McGraw-Hill Company, New York, 1972).
[9] Y. Gohar et al., Technical report for the ITER blanket/shield – A. Blanket, ITER-TN-BL-5-0-3 (July–November 1990).
[10] C.P.C. Wong et al., ARIES-I design final report, Chapter 8: Fusion-power-core engineering, UCLA-PPG-1323 (1991)
[11] M.C. Billone and W.T. Grayhack, Summary of mechanical properties data and correlations for Li_2O, Li_4SiO_4, $LiAlO_2$, and Be, ANL/FPP/TM-218 (1990).
[12] M. Fumizawa, M. Ogawa, M. Hishida, and K. Okamoto, Experimental study on helium–air exchange flow through a small opening, Proceedings of FLUCOME 91 (1991) 333–340.